Research Article

Therapeutic Potential of Andrographolide Isolated from the Leaves of *Andrographis paniculata* Nees for Treating Lung Adenocarcinomas

Yu-Tang Tung,[1] Hsiao-Ling Chen,[2] Hsin-Chung Tsai,[1,3] Shang-Hsun Yang,[4] Yi-Chun Chang,[1] and Chuan-Mu Chen[1,5]

[1] *Department of Life Sciences, Agricultural Biotechnology Center, National Chung Hsing University, Taichung 402, Taiwan*

[2] *Department of Bioresources, Da-Yeh University, Changhwa 515, Taiwan*

[3] *Taichung Hospital, Department of Health, Taichung 403, Taiwan*

[4] *Department of Physiology, National Cheng Kung University, Tainan 701, Taiwan*

[5] *Department of Life Sciences, Office of Research and Development, National Chung Hsing University, No. 250, Kuo Kuang Road, Taichung 402, Taiwan*

Correspondence should be addressed to Chuan-Mu Chen; chchen1@dragon.nchu.edu.tw

Andrographolide is one of the major diterpene lactones found in *Andrographis paniculata* Nees and exhibits remarkable inhibitory effects on various cancers. In this study, the antipulmonary cancer effects of andrographolide were studied in a lung tumor mouse model induced by human vascular endothelial growth factor A_{165} (*hVEGF*-A_{165}). These results demonstrated that andrographolide significantly reduced the expression of hVEGF-A_{165} compared with a mock group in the Clara cells of the lungs. In addition, andrographolide also decreased tumor formation by reducing VEGF, EGFR, Cyclin A, and Cyclin B expression on the transcriptional and translational levels. These results indicated that andrographolide treatment on the overexpression of VEGF can arrest the cell cycle, which induced pulmonary tumors in transgenic mice. In conclusion, the antiangiogenesis and chemotherapeutic potential of andrographolide may provide a cure for pulmonary tumors in the future.

1. Introduction

According to the latest cancer mortality statistics from the People's Health Bureau of Taiwan, pulmonary cancer is ranked as a leading cause of Taiwanese cancer-related deaths [1]. Worldwide, lung cancer has been the most common form of cancer for several decades. Although chemotherapeutic agents for pulmonary tumors have developed, the lung cancer death rate is still high. Thus, many researchers have focused on early tumor detection and more active treatments as the tumor prevention methods [2]. For example, many researchers have discovered useful phytochemicals (compounds found in plants) and phytochemicals derivatives that provide novel anticancer therapies that have been successfully used in the clinic.

Andrographis paniculata Nees, a traditional medicine in Southeastern Asian countries, has been widely used in the clinic as an immunostimulant [3] and for the treatment of the common cold [4], myocardial ischemia [5], pharyngotonsillitis [6], and respiratory tract infections [7]. The major component of *A. paniculata* is andrographolide, which has been used to treat colds, diarrhea, fever, and inflammation, as well as infectious diseases [8]. In addition, the chemopreventive effects against and the inhibitory effects on cancer cell growth of andrographolide have been demonstrated in breast, colon, epidermoid, gastric, liver, leukemia, myeloma, peripheral blood lymphocytes, and prostate cancers [9–12]. The present study is the first to investigate whether andrographolide treatment could inhibit the formation of lung tumor in the hVEGF-A_{165} overexpressing transgenic mice. The airway hyperresponsiveness (AHR) was measured during a five-month treatment of mice with andrographolide. In addition, the pathological histology and the hVEGF
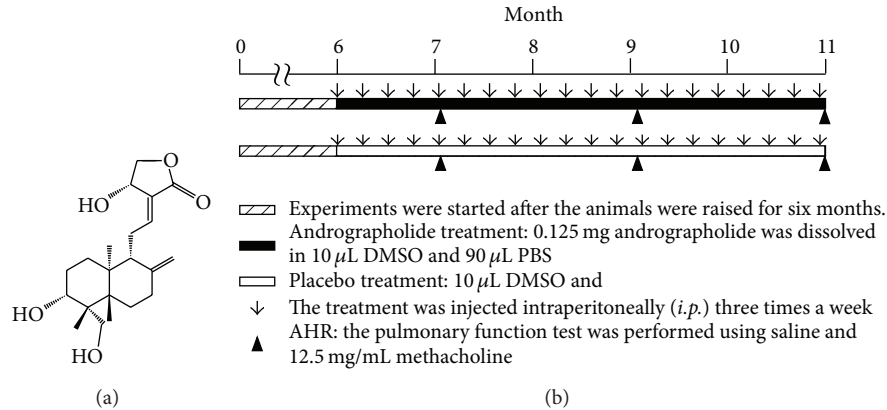
FIGURE 1: Active component of andrographolide (An) extracted from the leaves of *Andrographis paniculata* Nees and the animal trial timeline. (a) Chemical structure of andrographolide. (b) The schedule of andrographolide treatment. Mice were injected intraperitoneally (*i.p.*) with andrographolide (5 mg/kg body weight) three times a week for 5 months, and mice were sacrificed at 11 months.

immunohistochemistry staining of the lungs of these mice were examined. The related mRNA and protein expression in tumorigenesis and cell cycle regulator makers were also tested to evaluate the mechanism of tumor inhibition by treatment with andrographolide.

2. Materials and Methods

2.1. Production of Lung Tumor Transgenic Mice. We have generated the mccsp-hVegf-A_{165}-sv40 transgenic mice from pronuclear microinjection technique. Homozygous (hVEGF-$A_{165}^{+/+}$) or hemizygous (hVEGF-$A_{165}^{+/-}$) transgenic mice were identified by genomic DNA PCR. The genomic DNA isolated from the tails of the mice with the following primers: VEGF-94(+): 5′-AAGGAGGAGGGCAGAATCATC-3′ and VEGF-315(−): 5′-GAGGTTTGATCCGCATAATCTG-3′. The exogenic human VEGF-A_{165} protein and mRNA expression levels in homozygous (hVEGF-$A_{165}^{+/+}$) or heterozygous (hVEGF-$A_{165}^{+/-}$) transgenic mice were also detected by Western blot and RT-PCR.

2.2. Animals. A total of 12 male transgenic mice were given with free access to water and standard laboratory diet at a temperature- and humidity-regulated environment (22 ± 2°C, 65 ± 5% RH) with 12 h dark/light cycle. This study was conducted according to institutional guidelines and approved by the Institutional Animal Care and Utilization Committee of National Chung-Hsing, Taiwan (IACUC no. 96-83). The transgenic mice displaying the hemizygous (hVEGF-$A_{165}^{+/-}$) genotype were randomly divided into two groups ($n = 6$) based on their treatment: Tg/Mock (transgenic mice treated with a mock or placebo) and Tg/Andrographolide (transgenic mice treated with andrographolide). Andrographolide (An; Figure 1(a)) was obtained from Sigma Chemical (St. Louis, MO, USA) and dissolved in DMSO. Mice were injected intraperitoneally (*i.p.*) with andrographolide (5 mg/kg body weight) three times a week for 5 months, and mice were sacrificed at 11 months (Figure 1(b)). Pulmonary tissues were collected for pathological histology, immunohistochemistry

staining, RNA extraction, and protein extraction according to our previously published protocols [13–15]. All the experiments were repeated twice.

2.3. Measurement of the Airway Hyperresponsiveness (AHR). Bronchial provocation tests that evaluate the AHR in the Tg/Mock and Tg/Andrographolide groups were performed using methacholine. First, the basal pulmonary function was measured; then saline and methacholine at a concentration of 12.5 mg/mL were converted to aerosol using a nebulizer and allowed to be inhaled five times through a Rosenthal-French dosimeter. The pulmonary function was measured 30 times with a portable microspirometer for 3 minutes, and the enhanced pause (penh) values were selected to represent the pulmonary function. The penh, a dimensionless value, represents the proportion of maximal expiratory to maximal inspiratory box pressure signals and the timing of expiration. The AHR was presented as the penh in response to the increasing damage to pulmonary functionality [16].

2.4. Pathological Histology. Pulmonary tissues were fixed in 10% buffered formaldehyde (pH 7.0), embedded with paraffin, sectioned into 3 μm sections, and examined using hematoxylin and eosin (H&E) staining. The hematoxylin and eosin (H&E) staining was described according to our previous reports [17, 18].

2.5. Immunohistochemistry Staining. IHC staining of pulmonary tissues, the VECTASTAIN ABC kit (Universal, Vector, USA) was used. Tissue sections (a thickness of 5 μm) were placed on slides and incubated overnight at 4°C with rabbit anti-hVEGF-A monoclonal primary antibody as previously described [19]. Sections were developed using diaminobenzidine (DAB) as chromogenic substrates and counterstained with hematoxylin [20].

2.6. Real-Time RT-PCR. RNA was extracted from lung tissue using a Trizol reagent (Invitrogen, Carlsbad, CA) in accordance with the manufacturer's instructions. cDNA synthesis
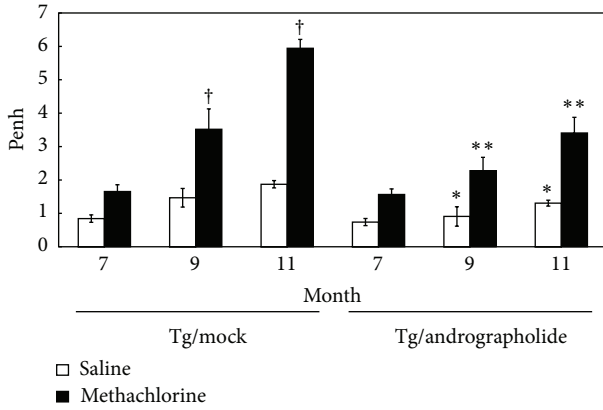
FIGURE 2: Effects of andrographolide on the airway hyperresponsiveness (AHR) parameters of pulmonary functionality. Data are presented as the means ± SEM ($n = 6$). $^{\dagger}P < 0.01$ Tg/Mock versus Tg/Mock group at 7 months. $^{*}P < 0.05$ Tg/Andrographolide group versus Tg/Mock group in the same month. $^{**}P < 0.01$ Tg/Andrographolide group versus Tg/Mock group in the same month.

TABLE 1: Lung tumorigenesis frequency of Tg/Mock and Tg/Andrographolide groups in the mouse lung tissues ($n = 6$) using histopathological image analysis.

Variable	Tg/Mock	Tg/Andrographolide
Normal	0 (0%)	2 (33.3%)
Cyst	6 (100%)	4 (66.7%)
Damaged alveoli	4 (66.7%)	2 (33.3%)
Mild emphysematous change	0 (0%)	3 (50%)
Prominent emphysematous change	6 (100%)	1 (16.7%)
Hemosiderin-laden macrophages in alveoli	2 (33.3%)	0 (0%)
Old hemorrhage	6 (100%)	2 (33.3%)
Moderate lymphocytic infiltration	0 (0%)	1 (16.7%)
Marked chronic lymphoid infiltration	6 (100%)	2 (33.3%)
Neoplasm	3 (50%)	1 (16.7%)
Lymphoma	6 (100%)	1 (16.7%)
Adenocarcinoma	5 (83.3%)	2 (33.3%)

reaction was performed by PCR as described for ImProm-IITM reverse transcriptase (Promega, USA). Quantitative real-time RT-PCR (qRT-PCR) was carried out using SYBR Green in a Rotor-Gene 6000. The gene expressions of 14 genes (*vegf, kdr, nrp-1, myc, brca-1, mmp2, mmp9, egfr, erk2, survivin, cyclin a, cyclin b1, cyclin d,* and *cyclin e*) were performed on using cDNA from pulmonary tissue by qRT-PCR [21].

2.7. Western Blotting. The total protein of the pulmonary tissues from each mouse was homogenized in 500 μL of RIPA buffer (5 mM Tris-HCl pH 7.4, 0.15 M NaCl, 1% NP40, 0.25% sodium deoxycholate, 5 mM EDTA, and 1 mM ethylene glycol-bis (2-aminoethyl-ether)-N,N,N,N-tetraacetic acid) and centrifuged at 12,000 ×g for 30 min at 4°C. Protein determination and Western blotting was performed according to the procedure reported [20, 22] with slight modifications. The protein samples (50 μg) were resolved by a 10% SDS-PAGE and electrophoretically transferred to a PVDF membrane. Thus, the membrane was incubated with primary antibody (VEGF-A, EGFR, ERK2, Cyclin A, Cyclin B, or GAPDH) overnight at 4°C and further incubated for 1 h with anti-rabbit IgG antibody conjugated to HRP. The protein expressions were detected by the enhanced chemiluminescence reagents (ECL).

2.8. Statistical Analysis. Statistical significance of differences between treatments was determined by Student's *t*-test. $P < 0.05$ (*) or $P < 0.01$ (**) were considered to be statistically significant.

3. Results

3.1. Effects of Andrographolide on the Airway Hyperresponsiveness (AHR) Parameters of Pulmonary Functionality. The mccsp-hVegf-A165-sv40 transgenic mice which induces pulmonary tumor [16] was used as a lung cancer animal model

for test of andrographolide (An) therapeutic effects. The animal trials timeline was showed in Figure 1(b). Several invasive and noninvasive methods have been used for the evaluation of the airway responsiveness of mice [23]. The AHR, a noninvasive procedure, enables easily and quickly obtained measurements, and it has been an important characteristic of pulmonary function. In this study, the AHR of the andrographolide or mock treatment was measured after 7, 9, and 11 months (Figure 2). The penh values of the Tg/Mock treatment with methacholine were significantly increased from 1.65 (7 months) to 3.52 (9 months), and 5.94 (11 months). However, 5 mg/kg body weight of andrographolide effectively reduced the penh elevation, exhibiting values of 1.57 (7 months), 2.28 (9 months), and 3.41 (11 months). This result revealed that andrographolide dramatically reduced the damage to pulmonary functionality.

3.2. Effect of Andrographolide Treatment on Lung H&E Staining and Pathological Analysis. Figure 3 and Table 1 indicate that transgenic mice (83.3%; 5/6) have found pulmonary tumors; these tumors primarily consisted of neoplasms growth on the periphery of the pulmonary alveolus and adenomas growing on the site near the lung bronchus. In the pulmonary alveoli of the lung bronchi of the transgenic mice, some obvious large-grained pink cells, which represent macrophages, are indicative of an inflammatory response. Furthermore, the group treated with 5 mg/kg andrographolide decreased the neoplasm growing on the periphery of the pulmonary alveolus and the adenomas growing near the site of the lung bronchus (Figures 3(c) and 3(d)). This pathological analysis illustrated that andrographolide has antipulmonary cancer potential (33.3%; 2/6) compared with Tg alone (83.3%; 5/6) and induces anti-inflammatory
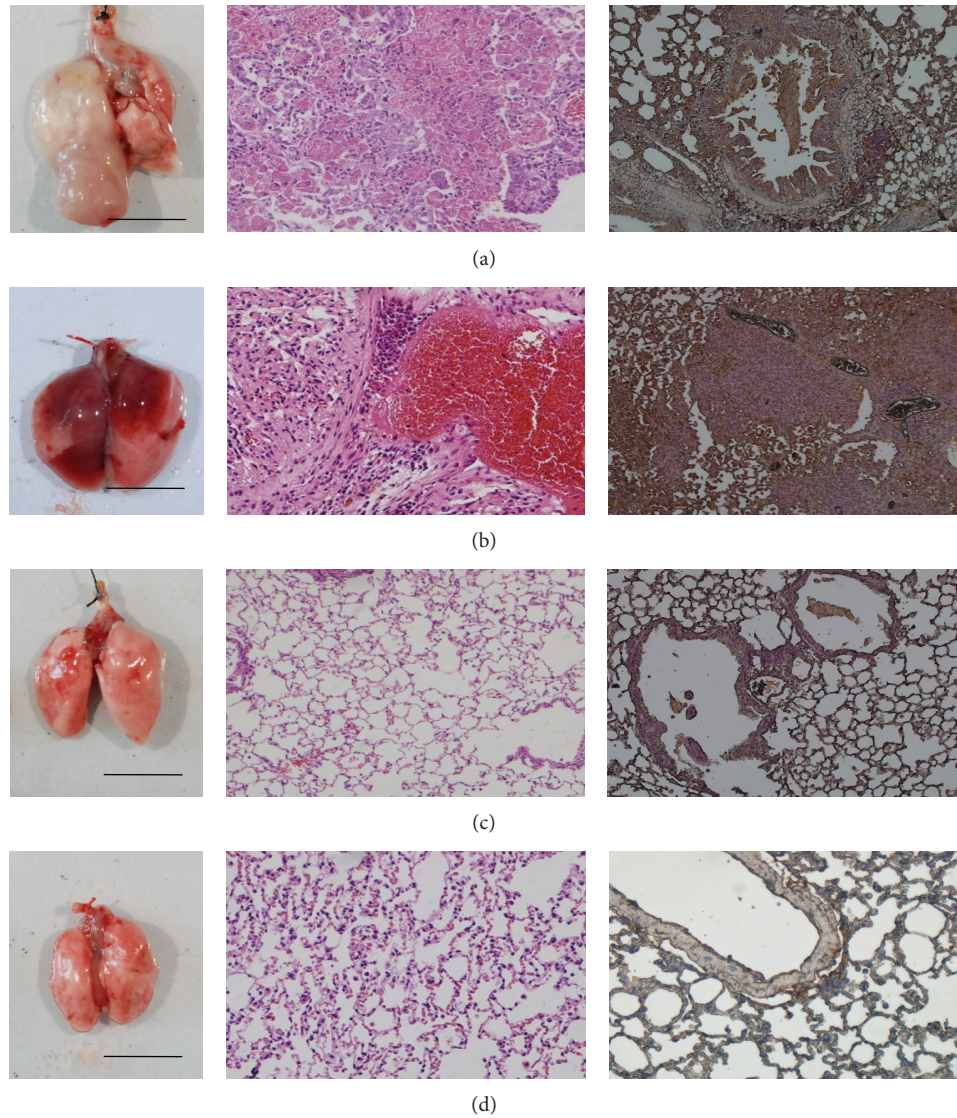
(a)

(b)

(c)

(d)

Figure 3: The exterior, histopathological slides and immunohistochemical (IHC) staining of the lung tissues of 11-month-old transgenic mice that overexpress hVEGF-A$_{165}$ in the (a, b) Tg/Mock group and (c, d) Tg/Andrographolide group following 5 months of andrographolide treatment.

responses in the lungs of transgenic mice that overexpress hVEGF-A$_{165}$.

3.3. Effect of Andrographolide Treatment on Immunohistochemistry Staining.
Angiogenesis is required for the tumor formation, tumor growth, invasion, and metastasis. VEGF is a principal regulator of vasculogenesis and angiogenesis. Using immunohistochemistry staining (IHC staining), we observed that VEGF was overexpressed in the Clara cells of lung tissues in the transgenic mice (Figures 3(a) and 3(b)) and that the treatment with andrographolide significantly reduced the expression levels of VEGF (Figures 3(c) and 3(d)). These results indicate that transgenic mice treatment with andrographolide can decrease VEGF expression compared with those that were mock treated; thus it may reduce the new blood vessel formation and growth. The anti-VEGF therapy of

andrographolide may prevent the previously observed tumor growth, invasion, and metastasis.

3.4. Andrographolide Suppresses the Marker Genes for Tumor Formation.
The mRNA levels of *vegf-a165*, *kdr*, *nrp-1*, *myc*, *brca-1*, *mmp2*, *mmp9*, *egfr*, *erk2*, *survivin*, *cyclin a*, *cyclin b1*, *cyclin d,* and *cyclin e* in the Tg/Mock and Tg/Andrographolide groups were evaluated using qRT-PCR (Figure 4). These results demonstrated that treating Tg mice with 5 mg/kg of andrographolide significantly decreased the expression of *vegf-a165*, *kdr*, *nrp-1*, *c-myc*, *egfr*, *erk2*, *surviving*, *cyclin a*, *cyclin b1,* and *cyclin e*. *Kdr* and its coreceptor *nrp-1*, which are the main angiogenic receptors in the vegf pathway, are down-regulated. In addition, both the c-Myc and Ras/MEK/ERK pathways play a vital role in the progression of the G1-cell cycle phase by enhancing cyclins. Thus, in this study *erk2*
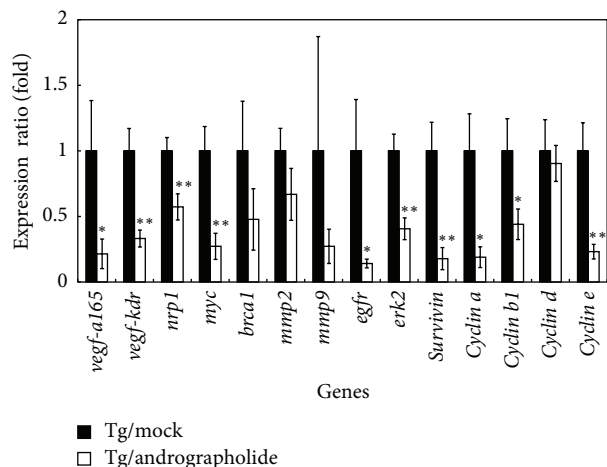
FIGURE 4: Real-time PCR validations of mRNA expression levels of *vegf*, *kdr*, *nrp-1*, *myc*, *brca-1*, *mmp2*, *mmp9*, *egfr*, *erk2*, *survivin*, *cyclin a*, *cyclin b1*, *cyclin d*, and *cyclin e* in the lung tissues of the Tg/Mock and Tg/Andrographolide groups. β-Actin was used as an internal control. The quantitative mRNA expression levels were measured by qRT-PCR. Data are presented as the means ± SEM ($n = 6$). $^{*}P < 0.05$ versus Tg/Mock group. $^{**}P < 0.01$ versus Tg/Mock group.

and c-myc down-regulation may induce cell cycle G1 arrest. Furthermore, *cyclin a* is essential for *c-myc*-modulated cell-cycle progression.

3.5. Andrographolide Suppresses Cell Cycle Progression Signaling Pathways. VEGF, ERK2, Cyclin A, and Cyclin B were significantly decreased in the Tg/Andrographolide group compared with the Tg/Mock group using Western blot analysis (Figure 5). Andrographolide affects the cell cycle by reducing the levels of Cyclin A and Cyclin B, which regulate the S and G2/M phases, respectively. The andrographolide-induced downregulation of Cyclins A and B may decrease the progression of cells through the S and G2/M phases. This result indicates that the protein expression involved in the S to M phase transition in transgenic mice was inhibited by andrographolide.

4. Discussion

Previous studies have shown that *Andrographis paniculata* possesses potent antiatherosclerotic, anti-inflammatory, antioxidant, hepatoprotective, immunomodulatory, and anti-cancer effects [24–29]. Andrographolide is one of the major diterpene lactones found in *A. paniculata* and displays potent anticancer and immunomodulatory effects, which may lead to its development as a chemotherapeutic agent [28, 30]. In addition, many researchers have demonstrated that andrographolide displays excellent anticancer effects on breast, colon, epidermoid, gastric, HeLa, liver, leukemia, myeloma, peripheral blood lymphocytes, and prostate cancers [9–12]. Many *in vitro* studies demonstrated that andrographolide promotes apoptosis in cancer cells, suppresses cancer cell proliferation, and induces cell-cycle arrest [12, 31].

The stabilization of HIF-1α mediated the overexpression of VEGF, which has been identified as a common step in the development of carcinomas. Thus, VEGF-inhibitors, which directly or indirectly target the tumor vasculature, have become common in anticancer therapies [32]. In the present study, we use 11-month-old transgenic mice that overexpress a lung-specific hVEGF-A$_{165}$. These mice contain the mccsp-hVegf-A$_{165}$-sv40 poly(A) transgene for researching pulmonary tumors and serve as an animal model for researching the regulatory mechanism of andrographolide. We found that these transgenic mice are susceptible to the growth of pulmonary tumors. However, following a 5-month treatment with andrographolide (5 mg/kg b.w. three times a week), these mice exhibited a dramatic decrease in the formation of solid tumors when compared with the mock treatment. The histological examination also indicated that the andrographolide treatment reduced pulmonary tumor formation and inflammation (Figure 3).

Initially, the cancer cells continue to proliferate and thus create a nutrition and oxygen deficiency, which causes significant cell death. The secretion of large quantities of VEGF-A$_{165}$ induces vasculogenesis to provide the rapidly growing tumor with sufficient quantities of nutrients and oxygen [33]. This solid tumor growth is dependent on angiogenesis, and thus the suppression of tumor blood vessels offers a new alternative to prevent and treat cancer. Using IHC staining, we observed that andrographolide reduced the expression of hVEGF-A$_{165}$ to normal levels, specifically in the Clara cells in the lungs of transgenic mice. These results indicate that andrographolide reduced the expression of VEGF in Clara cells when compared with the mock treatment. VEGF is essential for vasculogenesis and angiogenesis during development and tumor progression. In addition, Zhao et al. [34] demonstrated that andrographolide effectively inhibited VEGF expression in prostate cancer. Lin et al. [1] found that the inhibition of PI3 K/Akt signaling by andrographolide significantly suppressed the protein and mRNA levels of HIF-1α, as well as the protein level and transcriptional activation of VEGF in A549 cells. In this study, we further found that treatment with andrographolide in lung tumor animal model effectively reduced the expression of VEGF in tumor tissue; this activity demonstrates that andrographolide may prove a potent antiangiogenic agent for the treatment of pulmonary cancer.

In addition, andrographolide can reduce pulmonary functional damage (Figure 2) and prevent pulmonary cancer formation through elimination of VEGF, ERK2, Cyclin A, and Cyclin B proteins (Figure 5). Andrographolide induced the reduction of Cyclin A and Cyclin B, which likely resulted in the reduced progression through the S and G2/M phases. These results indicated that andrographolide suppressed the protein expression at the transition from the S-phase to the M-phase in transgenic mice. These results also demonstrate that the inhibition of the cell cycle may be a vital pathway that andrographolide affects the transgenic mice that overexpress VEGF. Furthermore, Satyanarayana et al. [12] revealed that andrographolide inhibits cell-cycle arrest in MCF-7 cells by inducing the expression of p27 (the cell-cycle inhibitory protein) and decreasing the expression of cyclin-dependent
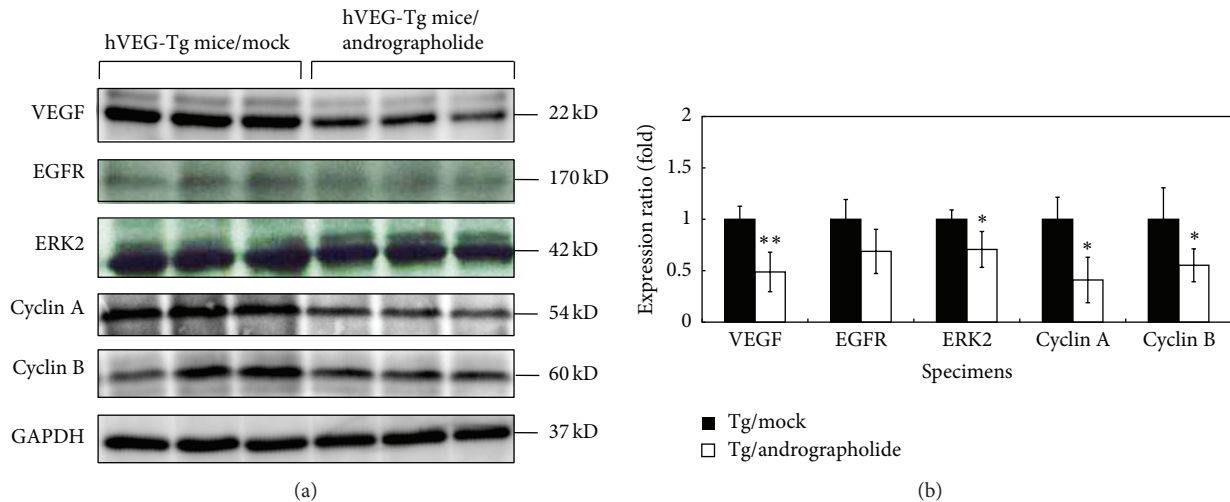
(a)   (b)

FIGURE 5: Western blot analysis of VEGF-A, EGFR, ERK2, Cyclin A, and Cyclin B protein in the lung tissues of the Tg and Tg/Andrographolide groups. GADPH was used as an internal control. Data are presented as the means ± SEM ($n = 6$). $^{*}P < 0.05$ versus Tg group. $^{**}P < 0.01$ versus Tg group.
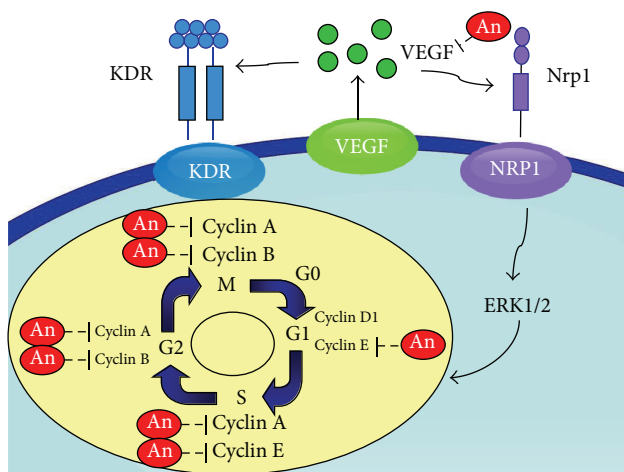

FIGURE 6: Scheme of the andrographolide regulatory pathway. The effects of andrographolide inhibition of lung tumors are hypothesized through a cell-cycle signaling pathway. The diagram shows that andrographolide may inhibit VEGF-A, KDR, Nrp1, ERK2, Cyclin A, and Cyclin B expression.

kinase. Shi et al. [31] also suggested that andrographolide can induce cell-cycle arrest at the G1/S phase by CKI-cyclin-Cdk signaling in Lovo cells. These results revealed that andrographolide can induce cell-cycle arrest in cancer cells. Furthermore, we found that *erk2* downregulation was followed by a downstream decreasing of *c-myc* expression that may induce cell cycle arrest in the G1 phase. Additionally, *cyclin a* is essential for *c-myc*-modulated cell-cycle progression in pulmonary cancer formation. Finally, Tsai et al. [18] found that andrographolide inhibited chemotic migration, which may be due to the inhibition of the ERK1/2 and Akt protein kinase cascades. Here we show a relationship between andrographolide treatment and the transcriptional

and translational levels of VEGF, EGFR, ERK2, and Cyclin A (Figure 6).

5. Conclusion

The andrographolide-induced inhibition of VEGF by arresting the cell cycle may be a critical mechanism for preventing pulmonary tumor angiogenesis and metastasis. The inhibition of VEGF by andrographolide may be a useful method for the chemoprevention of pulmonary cancer.

Abbreviations

AHR: Airway hyperresponsiveness
An: Andrographolide
DAB: Diaminobenzidine
H&E: Hematoxylin and eosin
IHC: Immunohistochemistry staining
Penh: The enhanced pause
qRT-PCR: Quantitative real-time RT-PCR
VEGF: Vascular endothelial growth factor.

Acknowledgments

References

[1] H.-H. Lin, C.-W. Tsai, F.-P. Chou et al., "Andrographolide downregulates hypoxia-inducible factor-1α in human non-small cell lung cancer A549 cells," *Toxicology and Applied Pharmacology*, vol. 250, no. 3, pp. 336–345, 2011.

[2] S.-S. Lin, K.-C. Lai, S.-C. Hsu et al., "Curcumin inhibits the migration and invasion of human A549 lung cancer cells through the inhibition of matrix metalloproteinase-2 and -9 and Vascular Endothelial Growth Factor (VEGF)," *Cancer Letters*, vol. 285, no. 2, pp. 127–133, 2009.

[3] A. Puri, R. Saxena, R. P. Saxena, K. C. Saxena, V. Srivastava, and J. S. Tandon, "Immunostimulant agents from *Andrographis paniculata*," *Journal of Natural Products*, vol. 56, no. 7, pp. 995–999, 1993.

[4] J. Melchior, S. Palm, and G. Wikman, "Controlled clinical study of standardized *Andrographis paniculata* extract in common cold-a pilot trial," *Phytomedicine*, vol. 34, pp. 315–318, 1996.

[5] G. Zhi-ling, Z. Hua-yue, and Z. Xin-hua, "An experimental study of the mechanism of *Andrographis paniculata* nees (APN) in alleviating the Ca2+-overloading in the process of myocardial ischemie reperfusion," *Journal of Tongji Medical University*, vol. 15, no. 4, pp. 205–208, 1995.

[6] V. Thamlikitkul, S. Theerapong, P. Boonroj et al., "Efficacy of *Andrographis paniculata*, nees for pharyngotonsillitis in adults," *Journal of the Medical Association of Thailand*, vol. 74, no. 10, pp. 437–442, 1991.

[7] J. T. Coon and E. Ernst, "*Andrographis paniculata* in the treatment of upper respiratory tract infections: a systematic review of safety and efficacy," *Planta Medica*, vol. 70, no. 4, pp. 293–298, 2004.

[8] Y.-C. Shen, C.-F. Chen, and W.-F. Chiou, "Andrographolide prevents oxygen radical production by human neutrophils: possible mechanism(s) involved in its anti-inflammatory effect," *British Journal of Pharmacology*, vol. 135, no. 2, pp. 399–406, 2002.

[9] Y. Tan, K. Chiow, D. Huang, and S. Wong, "Andrographolide regulates epidermal growth factor receptor and transferrin receptor trafficking in epidermoid carcinoma (A-431) cells: research paper," *British Journal of Pharmacology*, vol. 159, no. 7, pp. 1497–1510, 2010.

[10] C.-G. Jiang, J.-B. Li, F.-R. Liu, T. Wu, M. Yu, and H.-M. Xu, "Andrographolide inhibits the adhesion of gastric cancer cells to endothelial cells by blocking E-selectin expression," *Anticancer Research*, vol. 27, no. 4 B, pp. 2439–2447, 2007.

[11] N. P. Trivedi, U. M. Rawal, and B. P. Patel, "Hepatoprotective effect of andrographolide against hexachlorocyclohexane-induced oxidative injury," *Integrative Cancer Therapies*, vol. 6, no. 3, pp. 271–280, 2007.

[12] C. Satyanarayana, D. S. Deevi, R. Rajagopalan, N. Srinivas, and S. Rajagopal, "DRF 3188 a novel semi-synthetic analog of andrographolide: cellular response to MCF 7 breast cancer cells," *BMC Cancer*, vol. 4, article 26, 2004.

[13] H.-L. Chen, L.-C. Wang, C.-H. Chang et al., "Recombinant porcine lactoferrin expressed in the milk of transgenic mice protects neonatal mice from a lethal challenge with enterovirus type 71," *Vaccine*, vol. 26, no. 7, pp. 891–898, 2008.

[14] C.-J. Shen, W. T. K. Cheng, S.-C. Wu et al., "Differential differences in methylation status of putative imprinted genes among cloned swine genomes," *PLoS ONE*, vol. 7, no. 2, Article ID e32812, 2012.

[15] Y.-J. Chen, C.-Y. Wu, C.-C. Chang, C.-J. Ma, M.-C. Li, and C.-M. Chen, "Nuclear Krüppel-like factor 4 expression is associated with human skin squamous cell carcinoma progression and metastasis," *Cancer Biology & Therapy*, vol. 7, no. 5, pp. 777–782, 2008.

[16] Y.-T. Tung, H.-L. Chen, C.-W. Lai, C.-J. Shen, Y.-W. Lai, and C.-M. Chen, "Curcumin reduces pulmonary tumorigenesis in vascular endothelial growth factor (VEGF)-overexpressing transgenic mice," *Molecular Nutrition and Food Research*, vol. 55, no. 7, pp. 1036–1043, 2011.

[17] H.-L. Chen, Y.-W. Lai, C.-S. Chen et al., "Probiotic *Lactobacillus casei* expressing human lactoferrin elevates antibacterial activity in the gastrointestinal tract," *BioMetals*, vol. 23, no. 3, pp. 543–554, 2010.

[18] T.-C. Tsai, W. Lin, S.-H. Yang et al., "Granzyme G is expressed in the two-cell stage mouse embryo and is required for the maternal-zygotic transition," *BMC Developmental Biology*, vol. 10, article 88, 2010.

[19] C.-M. Chen, C.-M. Hung, C.-C. Yeh et al., "Gingyo-san enhances immunity and potentiates infectious bursal disease vaccination," *Evidence-Based Complementary and Alternative Medicine*, vol. 2011, Article ID 238208, 10 pages, 2011.

[20] C.-C. Yen, C.-Y. Lin, K.-Y. Chong et al., "Lactoferrin as a natural regimen for selective decontamination of the digestive tract: recombinant porcine lactoferrin expressed in the milk of transgenic mice protects neonates from pathogenic challenge in the gastrointestinal tract," *Journal of Infectious Diseases*, vol. 199, no. 4, pp. 590–598, 2009.

[21] J. Y. Chen, H. L. Chen, and J. C. Cheng, "A Chinese herbal medicine, Gexia-Zhuyu Tang (GZT), prevents dimethylnitrosamine-induced liver fibrosis through inhibition of hepatic stellate cells proliferation," *Journal of Ethnopharmacology*, vol. 142, pp. 811–818, 2012.

[22] S.-C. Wu, H.-L. Chen, C.-C. Yen et al., "Recombinant porcine lactoferrin expressed in the milk of transgenic mice enhances offspring growth performance," *Journal of Agricultural and Food Chemistry*, vol. 55, no. 12, pp. 4670–4677, 2007.

[23] V. L. Capelozzi, "Role of immunohistochemistry in the diagnosis of lung cancer," *Jornal Brasileiro de Pneumologia*, vol. 35, no. 4, pp. 375–382, 2009.

[24] H. M. Chang, *Pharmacology and Applications of Chinese Materia Medica*, vol. 2, World Scientific Publishing, Singapore, 1987.

[25] S. S. Handa and A. Sharma, "Hepatoprotective activity of andrographolide against galactosamine and paracetamol intoxication in rats," *Indian Journal of Medical Research Section B*, vol. 92, pp. 284–292, 1990.

[26] R. Ajaya Kumar, K. Sridevi, N. Vijaya Kumar, S. Nanduri, and S. Rajagopal, "Anticancer and immunostimulatory compounds from *Andrographis paniculata*," *Journal of Ethnopharmacology*, vol. 92, no. 2-3, pp. 291–295, 2004.

[27] T. Matsuda, M. Kuroyanagi, S. Sugiyama, K. Umehara, A. Ueno, and K. Nishi, "Cell differentiation-inducing diterpenes from *Andrographis paniculata* NEES," *Chemical and Pharmaceutical Bulletin*, vol. 42, no. 6, pp. 1216–1225, 1994.

[28] S. Rajagopal, R. A. Kumar, D. S. Deevi, C. Satyanarayana, and R. Rajagopalan, "Andrographolide, a potential cancer therapeutic agent isolated from *Andrographis paniculata*," *Journal of Experimental Therapeutics and Oncology*, vol. 3, no. 3, pp. 147–158, 2003.

[29] D. W. Wang and H. Y. Zhao, "Prevention of atherosclerotic arterial stenosis and restenosis after angioplasty with *Andrographis paniculata* nees and fish oil. Experimental studies of effects and mechanisms," *Chinese Medical Journal*, vol. 107, no. 6, pp. 464–470, 1994.

[30] S. R. Jada, A. S. Hamzah, N. H. Lajis, M. S. Saad, M. F. G. Stevens, and J. Stanslas, "Semisynthesis and cytotoxic activities of andrographolide analogues," *Journal of Enzyme Inhibition and Medicinal Chemistry*, vol. 21, no. 2, pp. 145–155, 2006.

[31] M.-D. Shi, H.-H. Lin, Y.-C. Lee, J.-K. Chao, R.-A. Lin, and J.-H. Chen, "Inhibition of cell-cycle progression in human colorectal carcinoma Lovo cells by andrographolide," *Chemico-Biological Interactions*, vol. 174, no. 3, pp. 201–210, 2008.

[32] L. Ellis, H. Hammers, and R. Pili, "Targeting tumor angiogenesis with histone deacetylase inhibitors," *Cancer Letters*, vol. 280, no. 2, pp. 145–153, 2009.

[33] N. Ferrara, "VEGF and the quest for tumour angiogenesis factors," *Nature Reviews Cancer*, vol. 2, no. 10, pp. 795–803, 2002.

[34] F. Zhao, E.-Q. He, L. Wang, and K. Liu, "Anti-tumor activities of andrographolide, a diterpene from *Andrographis paniculata*, by inducing apoptosis and inhibiting VEGF level," *Journal of Asian Natural Products Research*, vol. 10, no. 5-6, pp. 467–473, 2008.